Self-Regulated Complexity in Cultured Neuronal Networks

Eyal Hulata, Itay Baruchi, Ronen Segev, Yoash Shapira, and Eshel Ben-Jacob

School of Physics and Astronomy, Raymond & Beverly Sackler Faculty of Exact Sciences, Tel-Aviv University, Tel-Aviv 69978, Israel

(Received 7 August 2003; revised manuscript received 23 January 2004; published 14 May 2004)

New quantified observables of complexity are identified and utilized to study sequences (time series) recorded during the spontaneous activity of different size cultured networks. The sequence is mapped into a tiled time-frequency domain that maximizes the information about local time-frequency resolutions. The sequence regularity is associated with the domain homogeneity and its complexity with its local and global variations. Shuffling the recorded sequence lowers its complexity down to artificially constructed ones. The new observables are utilized to identify self-regulation motifs in observed complex network activity.

DOI: 10.1103/PhysRevLett.92.198105 PACS numbers: 87.18.Sn, 89.75.Hc, 05.45.Tp

Diverse open systems, biotic and abiotic alike, can exhibit complex dynamical behavior [1–8]. It has been suggested that the complexity of biotic systems can be inherently regulated via autonomous utilization of internally-stored means of control, hence, the term self-regulated complexity [8]. If correct, the complex activity of biotic cultured networks should be distinguishable from that of nonautonomous abiotic systems [9]. However, complexity is still an intuitive, blurred concept with no agreed-upon definition [1–8], so common quantified observables associated with it are yet to be developed. Towards this goal, we present a set of observables developed to capture some special features of the self-regulated activity of cultured networks. Specifically, our observables distinguish the latter from artificially constructed time sequences of similar statistical properties as well as the dynamics of modeled networks [10].

Hints about self-regulation in cultured networks.—Our *in vitro* networks were spontaneously formed from a mixture of cortical neurons and glia cells from one-day-old Charles River rats, homogeneously spread over a lithographically specified area (as detailed in [11,12]). Consequently, the spread cells turned into a network by sending dendrites and axons to form synaptic connections between neurons [11,12]. Although the above described self-wiring process is self-executed with no externally provided guiding stimulations or chemical cues, a relatively intense dynamical activity is spontaneously generated within several days. The activity is marked by the formation of synchronized bursting events (SBEs); each is a short ($\sim$200 ms) time window during which most of the recorded neurons participate in relatively rapid firing (Fig. 1). We illustrate in Fig. 1 that shuffling (random reordering of the intervals) alters the temporal ordering of the original sequence. However, as we have detailed in [11], such shuffling yet preserves the same statistical scaling properties (which can be approximated with the same Lévy distributions) [11,13] (and references within). In addition, the SBEs show long time correlations, and, for some networks, clear hierarchical temporal ordering (i.e., bursts of SBEs, bursts of bursts of SBEs, up to four detectable hierarchical levels) is observed [11]. Put together, the above observations motivated us to assume that the spontaneous activity of cultured networks might be self-regulated, despite the artificial nature of their construction. Such self-regulation can be executed via neuronal internal autonomous means, which are self-activated by the neurons. Or even more likely, they are coactivated by glia cells (with their own complementary regulatory means), which are coupled to the neurons [14,15].

Looking for quantified observables of self-regulated complexity.—Guided by the notion of self-regulated complexity (versus abioticlike nonautonomous complexity), we set to develop proper observables for distinguishing between these two possibilities. To proceed, we compare the recorded and shuffled sequences shown in Fig. 1. The recorded one is marked by large local and global temporal variations. Namely, at each temporal location, there are large frequency (density of SBEs) variations when looking at time windows of different widths. These local variations vary from place to place along the sequence. Guided by this realization and the previously mentioned special temporal features of the recorded sequences, we set the following requirements from our observables: (i) To associate the sequence regularity with the uniformity in the time-frequency (rates) relative resolutions rather than with the statistics of the temporal ordering.

FIG. 1 (color online). For the analysis of the temporal ordering of the network activity, it is convenient to convert the time series into a binary sequence, whose "1"s correspond to the SBEs and the width of the SBEs sets the basic time bin. Top: A 25 s long binary sequence representation of recorded SBEs. Bottom: The sequence after shuffling of the inter-SBE intervals.

The former refers to the relative resolution required to capture maximal information about the observed variations. (ii) To associate the sequence complexity with the local and global variations in the required relative resolutions instead of with the directly observed local and global frequency variations. (iii) To evaluate significantly lower values of complexities to the recorded sequences after they are shuffled, while keeping similar regularity regardless of shuffling. (iv) To be able to distinguish between the dynamical behaviors of different systems by their distinct positions on the complexity-regularity plane. (v) To be able to handle sequences with hierarchical temporal organizations.

Representation at the time-frequency plane.—To retain information about both temporal locations and frequency variations, we first transform the sequence into a presentation in its corresponding time-frequency domain utilizing the wavelet packets decomposition [16]. Next, we would like to extract at each temporal position (say the ith element of the sequence) information about the activity rates (frequencies) for all available time windows centered around this location. For a sequence of N_{bin} elements, the relevant time windows range from $\Delta t_{\mathrm{min}} \equiv 1$ (in units of the basic recording time width) to $\Delta t_{\mathrm{max}} \equiv N_{\mathrm{bin}}$. That is, we would like to extract information about N_{bin} time windows at each of the N_{bin} locations of the sequences. However, such N_{bin}^2 matrix for a sequence of only N_{bin} elements must contain redundant information (i.e., over-complete representation of the recorded sequence). In order to avoid such redundancy, only N_{bin} locations on the time-frequency domain are allowed to be selected, subject to the uncertainty constraint between time and frequency resolutions, $\Delta t \Delta f = 1$. Since there are also N_{bin} frequency bands, from $\Delta f_{\mathrm{min}} = 1$ to $\Delta f_{\mathrm{max}} = N_{\mathrm{bin}}$, it implies that each location can be assigned a local relative resolution $\Delta t/\Delta f$ out of $N_R = 1 + \log_2(N_{\mathrm{bin}})$ possible ratios (for simplicity, N_{bin} of the sequences considered here are in factors of 2).

It is convenient to illustrate both constraints as tiling of the time-frequency domain with N_{bin} rectangles, each with its own aspect ratio (height Δf and width Δt), representing the relative resolutions in time and frequency. We emphasize that the constraints are not simple Lagrange multipliers as the domain has to be covered with exactly N_{bin} nonoverlapping rectangles. Utilizing the wavelet-packet-decomposition algorithm allows partitioning (tiling) of the domain into rectangles of different aspect ratios. Each possible combination of N_{bin} nonoverlapping rectangles that geometrically covers the entire domain can serve as a complete basis that spans the recorded sequence on its corresponding time-frequency domain.

Selecting the best tiling.—The next challenge is to select, out of all possible tilings, the one which is most efficient in extracting the features of interest from the recorded sequence [16,17]. Here we are interested in a method that will generate for the recorded sequence and its shuffled version distinct tilings, as illustrated in Fig. 2. We follow the approach of Thiele and Villemoes [17], which is inspired by the notions of global Shannon information or Entropy minimization. The idea is to select the combination of rectangles that can capture most efficiently the information about local and global variations in the sequence temporal ordering. To do so, first, each possible rectangle is assigned a measure $M_n = -q_n \ln(q_n)$, where q_n is the normalized energy of the recorded sequence on the nth rectangle. The energy is evaluated for the case that the entire domain is tiled by the same rectangles (the same aspect ratio) as that of the nth rectangle. The global measure M—the summation of M_n over the N_{bin} rectangles—is utilized for selecting the best tiling; i.e., it is used as the cost function to be minimized. The algorithm presented in [17] is proved to minimize M. Examples of such best tilings for the recorded sequence and the shuffled one are shown in Fig. 2.

Evaluating the sequence regularity.— The sequence regularity R is usually perceived as a measure of its relative location on the abscissa between complete disordered (random) sequences ($R = 0$) and purely ordered (periodic) ones ($R = 1$). Several measures of regularity (e.g., algorithmic information content) have been suggested before [2,3]. These measures focus on the temporal locations of the events ("1") on the time axis. Here we present a new observable of regularity evaluated on the time-frequency domain. The idea is to associate the sequence regularity with the uniformity of its corresponding time-frequency domain, namely, with the uniformity of its rectangle distribution. The latter represents the distribution of the local relative resolutions in time and frequency as selected by the best tiling for extracting maximal information from the sequence.

From physics perspective, a tiled domain (Fig. 2) can be viewed as a magnetic material with the rectangles representing its local magnetizations. With this picture in mind, we first relate the local relative resolution of each rectangle n with its aspect ratio ($\Delta t/\Delta f$) by $R_n \equiv \log_2(\Delta t/\Delta f)/\log_2(N_{\mathrm{bin}})$. Defined this way, R_n (the

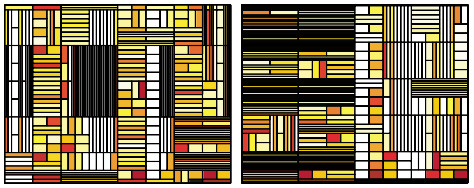

FIG. 2 (color online). Examples of best tiling for the recorded sequence (left) and its shuffled version (right), which are shown in Fig. 1. Time is on the horizontal axis and frequency on the vertical axis. The color levels represent the values of q_n. Note that for the shuffled sequence larger portions of the time-frequency domain are tiled by similar rectangles, which corresponds to weaker variations.

analogue of local magnetization) is assigned positive values for rectangles with higher frequency resolution (smaller Δf) and negative values for those with higher time resolution (smaller Δt). The normalization of R_n by the logarithm of the maximal aspect ratio N_{bin} entails that $-1 \leq R_n \leq 1$.

Next, drawing upon the notion of total magnetization, we simply define the sequence regularity R as the average of R_n. Defined this way, $R \cong 0$ for completely disordered sequences, i.e., sequences with Gaussian distribution of intervals, and $R \cong 1$ for purely regular ones, i.e., strings of one kind of interval. As will be shown later, artificial sequences constructed from the periodic and the random ends towards the center meet around $R = 0.5$. The regularity can also assign negative values for underdense (sparse) sequences in which the number of intervals is smaller than $\sqrt{N_{\mathrm{bin}}}$. Such sequences are not considered here.

Variation factors and Structural Complexity.—The regularity observable represents the uniformity of the time-frequency domain. Therefore, we set to define additional complementary observables associated with the domain varioformity. The latter refers to the distribution of local variations between neighboring rectangles. In order to capture the contribution of both local variations and their global variability between segments located at different positions, the sequence is segmented into words. For each word l, we define its variation factor VF to be

$$VF_l = \left(\frac{N_E(l) - \overline{N}_E}{\overline{N}_E}\right) \frac{\sum_{n,m} |R_n - R_m| \cdot \Theta(q_n \cdot q_m)}{\sum_{n,m} \Theta(q_n \cdot q_m)}, \quad (1)$$

where the sum is over all neighboring rectangles n, m. $N_E(l)$ is the number of events (and also intervals) detected within the lth word, and $\overline{N}_E$ is an average over different words of the same length as the lth one. $\Theta(x)$ is the Heaviside function; $\Theta(0) = 0$ and $\Theta(x \neq 0) = 1$.

Finally, in order to include also the variations between the sequence words, we identify the variance of the variation factors to be the sequence of its structural complexity SC. So that, for a sequence segmented into N_ω words, it is defined to be

$$SC \equiv \mathrm{var}(VF) \equiv \frac{1}{N_\omega} \sum_{l=1}^{N_\omega} (VF_l - \overline{VF})^2. \quad (2)$$

Exploring the complexity plane with test sequences.—In order to gain a better understanding of the relation between statistical scaling properties of the sequences (e.g., α, γ, and δ for sequences with Lévy distribution) and their locations on the complexity plane, we utilized artificially constructed families of sequences with different Lévy parameters. The construction of an artificial sequence is as follows. We draw a set of numbers out of a Lévy distribution generator with parameters α, γ, and δ. This set is then rounded and used as intervals between adjacent events. This sequence is a *realization* of the distribution, and there could be variations between different such realizations. Hence, for each set of Lévy parameters, we constructed 32 realizations, calculated R and SC for each of them, and use $\overline{R}$ and $\overline{SC}$ as the regularity and structural complexity. We have noticed that there was no difference between $\overline{R}$ and $\overline{SC}$ of the original and shuffled artificial realizations (within fractions of the deviations). That is not surprising as shuffling does not alter the distribution.

This procedure enables us to construct families of binary sequences, such that each family covers the entire range from disordered to purely periodic sequences, as illustrated in Fig. 3. Each family of sequences for a given α is composed of one branch on the random side ($R \lesssim 0.5$) for $\delta =$ "0" (minimum of one bin separation between events). On the regular side ($R \gtrsim 0.5$), each family has a unique branch for every $\delta \neq$ "0". The branches are spanned by varying γ, and they all meet for $\gamma \gg \delta$ at a location on the border between the random and regular sides and at relatively higher complexity (as shown in detail in Fig. 3).

Utilizing the complexity plane in search for self-regulation.—As shown, families of artificially constructed sequences exhibit very rich characteristics on the complexity plane. These characteristic maps can be utilized to identify features presumably related to self-regulation motifs of biotic systems. In Fig. 4 we show typical examples of the evaluated complexity/regularity for recorded and shuffled sequences, of spontaneous neuronal activity. Also shown is a corresponding, artificially constructed sequence with the same α, γ, and δ.

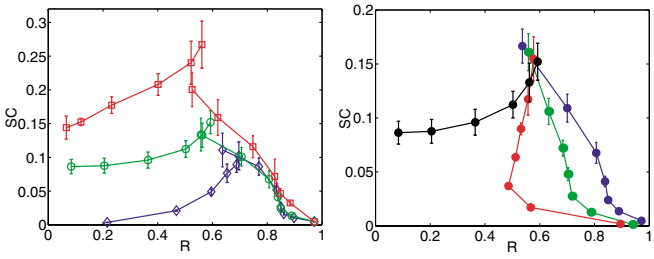

FIG. 3 (color online). Families of artificially constructed sequences with both zero-mean and finite-mean symmetric Lévy distributions of intervals. For each set of Lévy parameters (α, γ, and δ), we present $\overline{R}$ and $\overline{SC}$, using std(R) and std(SC) as error bars (<13%). Left: $\alpha = 2.0$; 1.6 and 1.2 on both random and regular sides ($\delta = 0$ and $\delta = 20$). γ spans the characteristics: for random ones, low regularity is observed at $\gamma = 1$ and higher regularity and complexity with increasing γ. For regular sequences, $\gamma = 1$ corresponds to high regularity ($R \to 1$) and higher γ lowers the regularity while increasing the complexity. For a given α, the regular branches meet the random branch at high complexity and intermediate regularity. Right: The behavior of the regular branches for the same α and different $\delta = 0, 5, 10, 20$. Note that all the regular branches meet together at the same location where the random branch crosses.

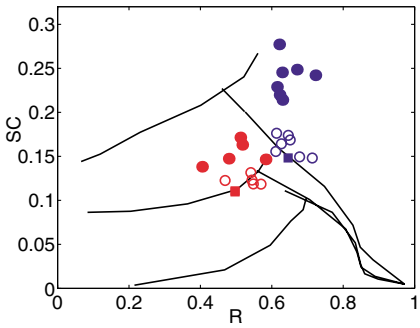

FIG. 4 (color online). Utilizing the complexity plane to study recorded activity. The solid lines are from Fig. 3. The dark solid dots represent different segments of *in vitro* recorded activity (over the course of an hour), $\overline{SC} = 0.24$ (std 0.02). The dark, open circles are the means of 5 different shufflings of each of the segments, $\overline{SC} = 0.16$ (0.01). The dark, solid rectangle is the mean of artificially constructed sequences with the same parameters [11], $\overline{SC} = 0.15$ (0.07). The statistical p values of recorded versus shuffled is 1×10^{-8}, recorded versus artificial is 1.8×10^{-3}, and shuffled versus artificial is 0.76. Using light open and solid circles, we present the same set for a different experiment [correspondingly, $\overline{SC} = 0.15$ (0.01), $\overline{SC} = 0.12$ (5×10^{-3}), and $\overline{SC} = 0.11$ (0.01); p values: 1.6×10^{-3}, 1.4×10^{-4}, and 0.41].

While these three types of sequences have very similar regularity, the recorded ones have significantly higher complexity than the shuffled sequences—as is clearly seen in the figure. Moreover, the complexity of the shuffled sequences is very similar to that of artificially constructed ones with matching Lévy parameters—the typical difference is within the standard deviation among different realizations. We studied ten different networks (one of 10^2 neurons, three of 10^4, and six of 10^6), each prepared from a different mixture of animal cells. For each network, we analyzed 12 sequences of 4096 bins. The number of SBEs per sequence ranges between 100–400, which is sufficient for the required statistics (SBEs $> \sqrt{N_{\text{bin}}}$). In addition, all tested sequences appeared to be located not at arbitrary locations on the complexity plane, but at special positions where the branches from the order and disorder sides cross. We propose that the above might reflect self-regulation of the activity, whose measure can be associated with the change in complexity upon shuffling the sequence while the regularity is sustained. In this regard, we also found that the complexity of simulated, modeled network dynamics (abiotic nonautonomous) does not change upon shuffling, and its regularity-complexity values are similar to those of artificially constructed sequences with matching parameters. We note that the modeled networks are composed of neurons with dynamical threshold connected via presynaptic dynamics, but lack additional inherent regulation, e.g., by glia cells [10].

Concluding remarks.—We found that, for hierarchical sequences, the variance of the VF exhibits a maximum for a specific word length. This time window defines the time width of the bursts of SBEs. It also serves as the time bin for construction of the binary sequence for the next level, in which an event ("1") is a burst of SBEs. Thus, the approach presented here can be extended for quantifying also the notion of functional complexity, which refers to the cross regulations of the dynamical activities at different levels [6,8]. For that we can evaluate the changes of the position on the complexity plane of a given level as induced by another one.

We thank A. Ayali, E. Fuchs, and N. Raichman for stimulating conversations. E. H. thanks A. Averbuch and R. Coifman for advising about best tiling. E. B. J. thanks S. Edwards, I. Procaccia, P. Hohenberg, and W. Kohn for illuminating questions and criticisms. Partial support received from the Adams Supercenter, the Kodesh Institute, and the ISF.

[1] B. A. Hubermann and T. Hogg, Physica (Amsterdam) **22D**, 376 (1986).
[2] M. Gell-Mann, *The Quark and the Jaguar* (Freeman, New York, 1994).
[3] R. Badii and R. Politi, *Complexity, Hierarchical Structures and Scaling in Physics* (Cambridge University Press, Cambridge, England, 1997).
[4] N. Goldenfeld and L. P. Kadanoff, Science **284**, 87 (1999).
[5] M. A. Jimenez-Montano *et al.*, BioSystems **58**, 117 (2000).
[6] E. Ben-Jacob and H. Levine, Nature (London) **409**, 985 (2001).
[7] T. Vicsek, Nature (London) **418**, 131 (2002).
[8] E. Ben-Jacob, Philos. Trans. R. Soc. London A **361**, 1283 (2003).
[9] Biotic/abiotic refers here to systems composed of living/artificial components. Correspondingly, autonomous/nonautonomous refers to the ability/inability of the system to regulate its activity, for example, calcium waves in glia fabrics, where the reaction is regulated by intracellular control of ionic channels versus chemical waves on platinum surfaces in a catalytic converter.
[10] V. Volman, I. Baruchi, E. Persi, and E. Ben-Jacob, Physica A (Amsterdam) (to be published).
[11] R. Segev *et al.*, Phys. Rev. Lett. **88**, 118102 (2002).
[12] R. Segev, M. Benveniste, Y. Shapira, and E. Ben-Jacob, Phys. Rev. Lett. **90**, 168101 (2003).
[13] H. E. Stanley *et al.*, Physica (Amsterdam) **270A**, 309 (1999).
[14] P. R. Laming *et al.*, Neurosci. Biobehav. Rev. **24**, 295 (2000).
[15] C. E. Stout *et al.*, J. Biol. Chem. **277**, 10 482 (2002).
[16] R. R. Coifman, Y. Meyer, and M.V. Wickerhauser, *Wavelets and their Applications* (Jones and Barlett, Boston, 1992).
[17] C. Thiele and L. Villemoes, Appl. Comput. Harmon. Anal. **3**, 91 (1996).